TECHNICAL DIVISION
SAVANNAH RIVER LABORATORY

DPST-82-490

DISTRIBUTION

J. A. Kelley
E. L. Albenesius
J. F. Ortaldo
L. M. Papouchado
F. H. Brown
M. D. Boersma
D. C. Witt
R. B. Ferguson
H. H. Elder
H. H. Hull
D. J. Pellarin
P. D. Soper
W. N. Rankin
N. E. Bibler
G. G. Wicks
D. F. Bickford
TIS File Copy (2)

This document was prepared in conjunction with work accomplished under Contract No. DE-DE-AC09-76SR00001with the U.S. Department of Energy.

DISCLAIMER

TECHNICAL DIVISION
SAVANNAH RIVER LABORATORY

DPST-82-490

MEMORANDUM

April 27, 1982

TO: M. J. PLODINEC

FROM: J. L. KESSLER

TIS FILE
RECORD COPY

EFFECT OF COOLING RATE, THERMAL EXPANSION, AND WASTE LOADING ON GLASS FRACTURE

INTRODUCTION AND SUMMARY

When waste glass is poured into metal canisters, it fractures primarily due to temperature gradients induced during cooling. It is desirable to minimize glass fracture (and thus glass surface area) to minimize release rates of radionuclides after disposal of the waste glass in a repository. It is difficult to predict the amount of fracture in a full-scale canister, since the effects and interactions of such variables as cooling rate, thermal expansion and waste loading are not yet well understood. A simple factorial experimental design has been used to determine the relative importance of these variables.

These results show using 8-inch diameter canisters that

- Slowing the cooling rate (by canister insulation) had the largest effect on glass cracking (approximately 2X). Thus, future tests designed to minimize cracking should concentrate on optimizing the cooling rate.
- Reducing the coefficient of expansion decreased the amount of cracking slightly, as did varying waste loading or content.
- Filling canisters off-center greatly increased the amount of fracture.

A technique to quantitatively determine the additional glass surface area due to fracture was developed based on this study. It should be applicable to glass forms of any size.

DISCUSSION

On October 12-14, 1981, thirteen 8-inch diameter carbon steel canisters were each filled with 100 lbs of glass at the Ferro Corporation in Cleveland, Ohio. Three glass fracture variables, cooling rate, thermal expansion and waste loading were tested in a two level factorial experimental design. This requires 8 cans of glass. The other five canisters were used to determine the temperature profile within the canister and the affect of extreme waste compositions. Table 1 gives the experimental conditions for each canister. The first three cans, #1-3, were instrumented with 10 type K thermocouples, 5 descending the centerline and 5 along the canister surface. These were used to determine the temperature profile in the canister during cooling and also the pour rate necessary to keep the canister temperature below 750°C. Maintaining the temperature below 750°C was necessary to avoid a phase change (and coefficient of expansion change) in the carbon steel. The 10 remaining canisters contained only one thermocouple located near the midline on the canister surface. Figures 1 and 2 show the dimensions of the cans and the location of the thermocouples.

In the simple factorial design, each variable had a high and a low value. The cooling rate was varied by varying the thickness of kaowool® insulation surrounding the canister. No insulation and 1 inch insulation were used. Thermal expansion coefficient was varied by varying the frit composition (Frits 131 and 142) with coefficients of expansion of 110 X 10^{-7}/°C and 88 X 10^{-7}/°C. Waste loadings of 0 and 28 wt % oxides were used. The composition of each frit and the different wastes are shown in Table 2.

Each glass batch was poured from a gas-fired cylindrical furnace. Homogeneity of the glass was assured by a constant rotation of the furnace during melting. Each canister required an individual feed charge because of the low furnace capacity (only 100 lbs). Melt flushes of 50 lbs were used between glass batches of different composition. The pour temperature was kept at 1000°C for each pour.

Since pour rate was not a variable in this experiment, all cans were poured at a rate which would just keep the canister temperature below 750°C. For uninsulated cans, this was only about 1 hour. Insulated cans (1 inch), however, required an average pour time of 2-1/2 hours. Thus, the corresponding pour rates are 100 lbs/hr and 40 lbs/hr. The latter was very near the lower limit at which the furnace could pour at a glass temperature of 1000°C.

Cooling Curves

A 40 channel data logger was used to record time and temperature data for each can. The first 3 canisters were used to determine pour rates to avoid a phase change in the steel. A second purpose was to determine temperature profiles in the can. Figures 3-8 show the cooling curves, both down the center of the glass and along the canister surface. The y axis, T-Ta, is the temperature difference as compared to ambient (Ta). Three thermocouple readings at 2, 10, and 18 inches are given in each figure to show a bottom, middle, and top reading. As expected, the uninsulated cans cooled much faster than the insulated. There was also a large difference between surface and centerline temperatures for the uninsulated can. Figure 9 shows the center to surface temperature difference (ΔT) for all 3 cans at the center height (TC #3&8). The arrow indicates the end of pour for each can. After pouring was complete, the uninsulated can still had a 300°C ΔT, while the insulated can had only a 25 and 50°C ΔT. This is a very significant point since the ΔT is believed to be the largest contributor to the extent of glass fracture.

Cooling curves for the remaining cans are shown in Figures 10-12. They are presented in three separate groups-insulated, uninsulated, and extreme waste compositions. All members of each group followed a very similar cooling pattern. This indicates that the amount of insulation had a common effect on glass temperature regardless of glass composition.

Glass Fracture

After the canisters had cooled, each canister was sectioned into four pieces as shown in Figure 13. This produced 2 radial cuts and 2 axial cuts. The latter were nearly mirror images of each other. Canisters were cut slowly (8 hours per canister) to insure that the cutting did not add to the amount of glass fracture.

To quantify the amount of cracking in each canister, photographs of each section were used to measure the crack length on each cut surface. The photographs were placed on an image analyzer grid and by tracing over the cracks the total crack length for each photograph was obtained. This value was then scaled from the canister area in the photograph to the actual canister area to obtain the crack length on each canister section. (As is shown later, the ratio of crack length to section area is proportional to the amount of additional surface area per unit volume.)

The results are shown in Table 3. For each can the length of cracks in each section is given as well as a total which is the sum of all four lengths. The total will be used to compare glass fracture because it should accurately represent the relative amount of cracking in each canister.

By examining the total cracking for each can it is readily apparent that slow cooling (insulation) can reduce the amount of cracking very substantially. Canister #4 is the only exception. However, examination of the photographs of this canister show that the glass was inadvertently poured near the canister wall and not in the center as for all other cans. This produced unsymmetrical temperature profiles in the glass and resulted in excessive glass fracture. Consequently, this canister was disregarded in the analysis. All other insulated cans had total crack lengths of less than 1600 cm. Uninsulated cans, on the other hand, all contained a much larger value (>2400 cm).

Table 4 shows the results of the factorial design which includes can #3, 5-9, 12, and 13. The results are recorded as the percent increase in crack length of the given variable as compared to its opposite under identical conditions. The design produces 4 comparisons for each variable with numbers in parenthesis indicating which cans were compared.

As the table shows, insulated cans were an average of 44% less cracked than noninsulated cans while frit type and waste loading had a much smaller effect. Frit 131 with a larger coefficient of expansion seemed to produce more cracking on cooling, but the effect was much less pronounced than that of insulation. The same was true of waste loading.

Many canister sections also contained voids. Figure 14 shows the void spaces in an axial section of can #6. As the photograph shows, most of the voids are near the center of the can where freezing of the glass occurs last. The surface area due to voids were measured by tracing the perimeter of each void on the image analyzer. The sum of all voids was scaled to the canister size. The results are shown in Table 5. Slow cooling (insulation) is the only factor which affected the amount of surface area due to voids. Insulated cans produce up to 10X more surface area due to voids than uninsulated canisters. However, the surface area increase from voids averages 5X smaller than that generated by fracture.

Quantifying Fracture

To help determine release rates of hazardous materials contained in the glass it is necessary to know the amount of

surface area generated by fracture. Direct measurement of surface area is impractical due to the irregularity of the size and shape of the fractured pieces and the likelihood that such a measurement would induce additional fracture. An alternate method is to section each canister into disks, measure the crack length on each surface by using a technique similar to that used here with the image analyzer and use the following approximation to determine the generated surface area.

$$S = \sum_{i=1}^{n} 2\, l_i dx_i \qquad (1)$$

where S = surface area generated
dx_i = width of each disk
l_i = length of cracks measured on each disk
n = number of sections

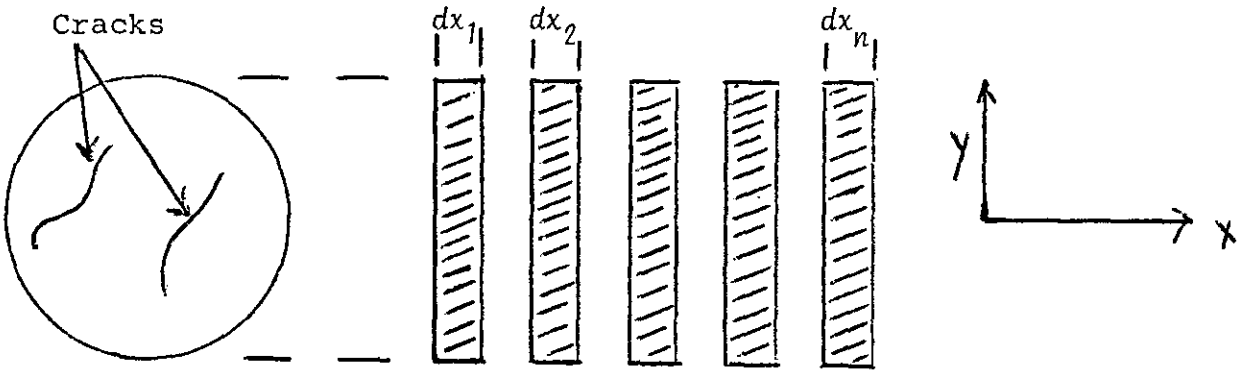

This assumes that the crack length in any radial plane of a particular disk is the same as the crack length on the surface of that disk. If this assumption is correct, then equation 1 merely calculates the surface area in each disk and then sums them to produce the surface area generated from fractures within the glass. The error in this measurement depends upon the number of disks which are measured. As the canister is sectioned into more disks, the width of each disk is smaller and the error of measurement gets smaller. Thus, it would be advantageous to section a canister into as many disks as possible. This approaches the exact equation of the surface area which is an integral.

$$S_e = \int_0^L 2\, l(x)\, dx \qquad (2)$$

where S_e = exact surface area generated
L = length of the canister
$l(x)$ = crack length on the radial plane at any point x along the axis

Because we do not know the crack length in each radial plane as a function l(x) of the axial distance (x), we cannot obtain the exact generated surface area. The best that can be done is to use Equation 1. In Table 3 the crack length of two radial sections for each canister is given. Table 6 shows the results assuming the average of the two is the average over the entire 20 inches of the canister. The relative surface area (RSA) is the surface area due to fracture divided by the monolith surface area. It depends on both the diameter and length of the can, and thus values obtained here will be different than those for full-sized canisters. The largest value is 11.1 for can #7. Also given is the surface area generated per unit volume (cm^{-1}). These values range from 0.8 to 2.6. Full-sized canisters with an RSA of 25 would have a surface area/volume of 1.9 cm^{-1}. The results are similar, indicating that the glass is fracturing into similar sized pieces for both the 8" diameter can and the full-sized can.

CONCLUSIONS

Small-scale tests on 8-inch diameter canisters show that slow cooling (insulation) can substantially reduce the amount of glass fracture in canisters and that thermal expansion and waste loading have only minor effects. Although canister size is a factor affecting glass fracture, it seems reasonable that insulation of full-sized canisters would also significantly reduce the amount of fracture. Although the trends are small on 8 inch cans, data also indicate less fracture with lower thermal expansion. On large cans with increased diameters the results could be significant and would indicate the use of a frit with a lower coefficient of thermal expansion.

To determine release rates of glass components, an effective method of measuring glass surface area from fracturing is needed. By sectioning canisters into disks the crack length on the surface of each disk can be used to determine the generated surface area. This procedure was demonstrated in this report and can be used on canisters of any dimension.

PROGRAM

The factorial design has the disadvantage of only testing two values for each variable. Trends between or beyond these values can only be inferred. Since the slower cooling rate decreased fracture very significantly in this test, additional tests should attempt to optimize this variable to further reduce the amount of glass fracture. These tests should examine cooling rates which are both slower and faster than that for 1 inch of insulation.

Pouring conditions were not varied in this study, but it seems likely that variables such as pour rate and temperature might also affect glass fracture. Therefore, in further tests varying pouring conditions and modes should also be examined.

TABLE 1

Experimental Conditions

Can #	Cooling Rate (Insulation Thickness (in)	Thermal Expansion (Frit Type)	Waste Loading (Wt %)
1*	3	131	0
2*	0	131	0
3*	1	131	0
4	1	131	0
5	0	131	0
6	1	131	28
7	0	131	28
8	1	142	0
9	0	142	0
12	1	142	28
13	0	142	28
10	1	131	28 (HiFe)
11	1	131	28 (HiAl)

*TC instrumented can

TABLE 2

Component	Frit 131 (Wt %)	Frit 142 (Wt %)
SiO_2	57.9	66.0
B_2O_3	14.7	14.2
Na_2O	17.7	12.3
Li_2O	5.7	3.8
MgO	2.0	0.9
TiO_2	1.0	1.9
La_2O_3	0.5	---
ZrO_2	0.5	0.9

Component	TDS (Wt %)	High Fe	High Al
Fe_2O_3	49.2	65.6	15.7
Al_2O_3	10.7	1.5	54.0
MnO_2	13.0	4.4	12.9
$CaCO_3$	6.1	4.4	1.0
NiO	5.7	11.2	2.3
$NaNO_3$	3.2	---	---
Na_2SO_4	1.3	2.5	2.3
Zeolite*	9.7	9.4	9.1
Anthracite Coal	1.0	1.0	1.0
SiO_2	---	---	1.7

*Linde Ion Siv IE-95

TABLE 3

Length of Cracks

Can #	Axial #1 (cm)	Axial #2 (cm)	Top Radial (cm)	Bottom Radial (cm)	Total (cm)
1*	420	441	96	171	1128
2	961	970	417	388	2736
3*	492	488	201	201	1382
4*	1067	1059	331	153	2610
5	922	929	324	227	2402
6*	551	570	227	195	1543
7	1316	1234	---	424	3398
8*	633	588	130	152	1503
9	996	873	241	278	2388
12*	613	543	183	154	1493
13	947	1077	332	349	2705
10*	596	585	204	129	1515
11*	571	560	122	169	1422

---No value taken, assume value is the same as other radial cut.
*Insulated.

TABLE 4

Relative Decrease in Surface Area Due To

Slow Cooling (%)		Low Coefficient of Expansion (%)		No Waste (%)	
42	(3.5)	8	(3.0)	10	(3.6)
55	(6.7)	0.6	(5.9)	42	(5.7)
37	(8.9)	3	(6.12)	0.7	(8.12)
45	(12.13)	26	(7.13)	13	(9.13)
Average = 44%		9%		16%	

TABLE 5

Surface Area Due to Voids

Canister	Void Perimenter**
1*	298
2	181
3*	528
4*	450
5	121
6*	748
7	33
8*	770
9	59
12*	528
13	66
10*	181
11*	419

*Slow-cooled, one-inch of insulation.
**Surface area is proportional to void perimeter.

TABLE 6

Surface Area Generated

Can *	Surface Area $(cm)^2$/Canister	RSA	Surface/Volume (1/cm)
1	13600	3.5	0.8
2	40900	10.5	2.5
3	20400	5.2	1.2
4	24600	6.3	1.5
5	28000	7.2	1.7
6	21400	5.5	1.3
7	43100	11.1	2.6
8	14300	3.7	0.9
9	26400	6.8	1.6
12	17100	4.4	1.0
13	34600	8.9	2.1
10	16900	4.3	1.0
11	14800	3.8	0.9

Can Volume = 16500 cm^3
Monolith Surface = 3890 cm^2

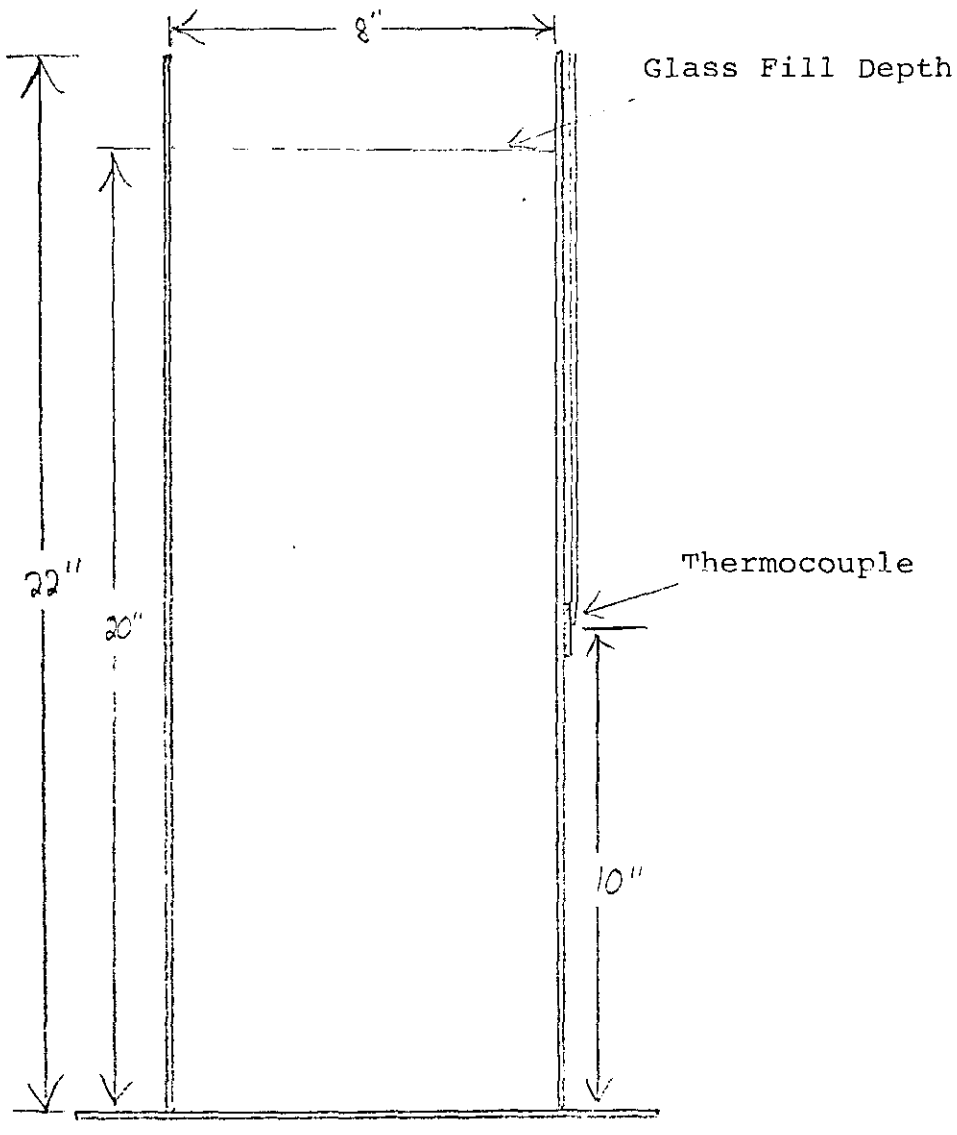

FIGURE 1. Canister Dimensions

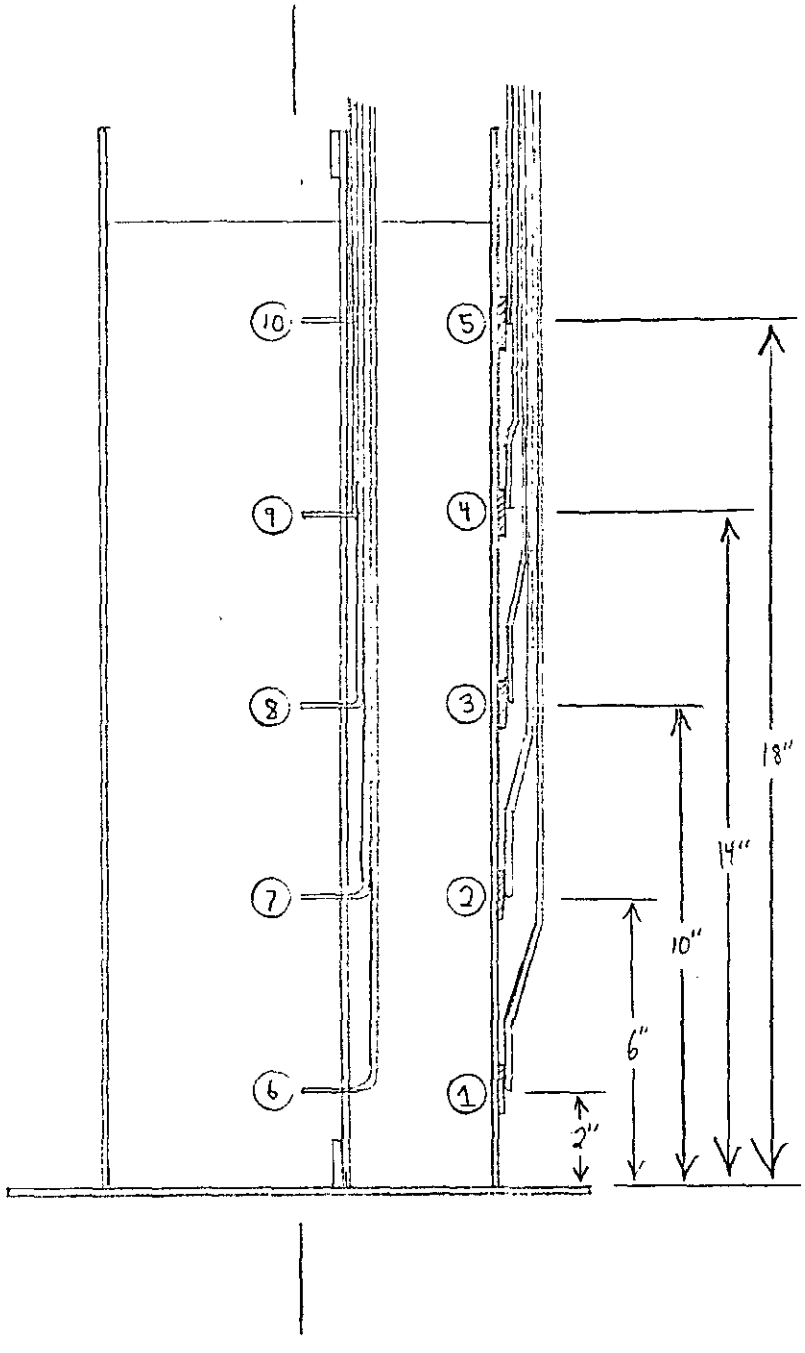

FIGURE 2. Instrumented Canisters

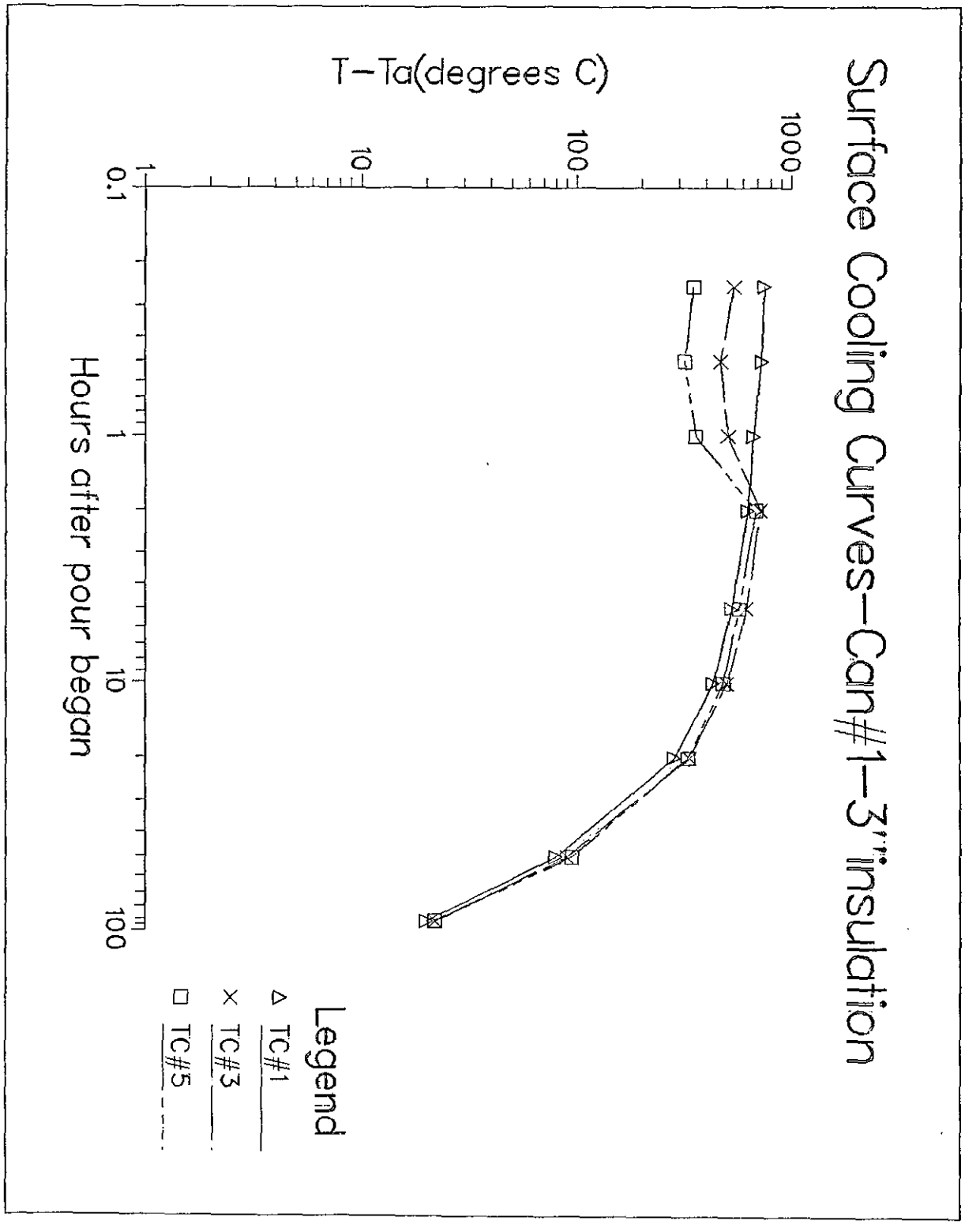
Surface Cooling Curves-Can#1-3"insulation
T-Ta(degrees C)
1000
100
10
1
0.1
Hours after pour began
1
10
100
Legend
TC#1
TC#3
TC#5

FIGURE 3

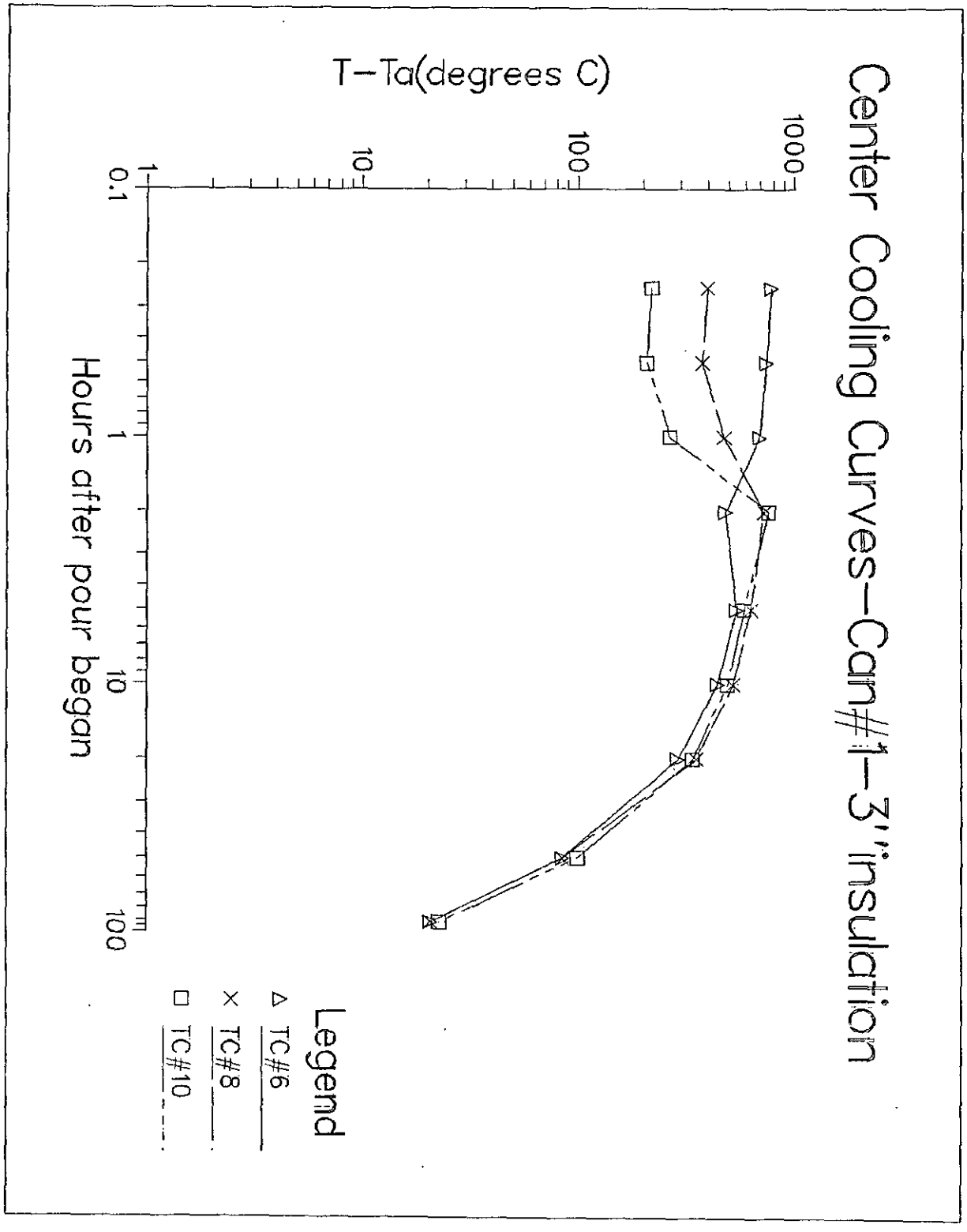
Center Cooling Curves-Can#1-3" insulation
T-Ta(degrees C)
1000
100
10
1
0.1
Hours after pour began
1
10
100
Legend
TC#6
TC#8
TC#10

FIGURE 4

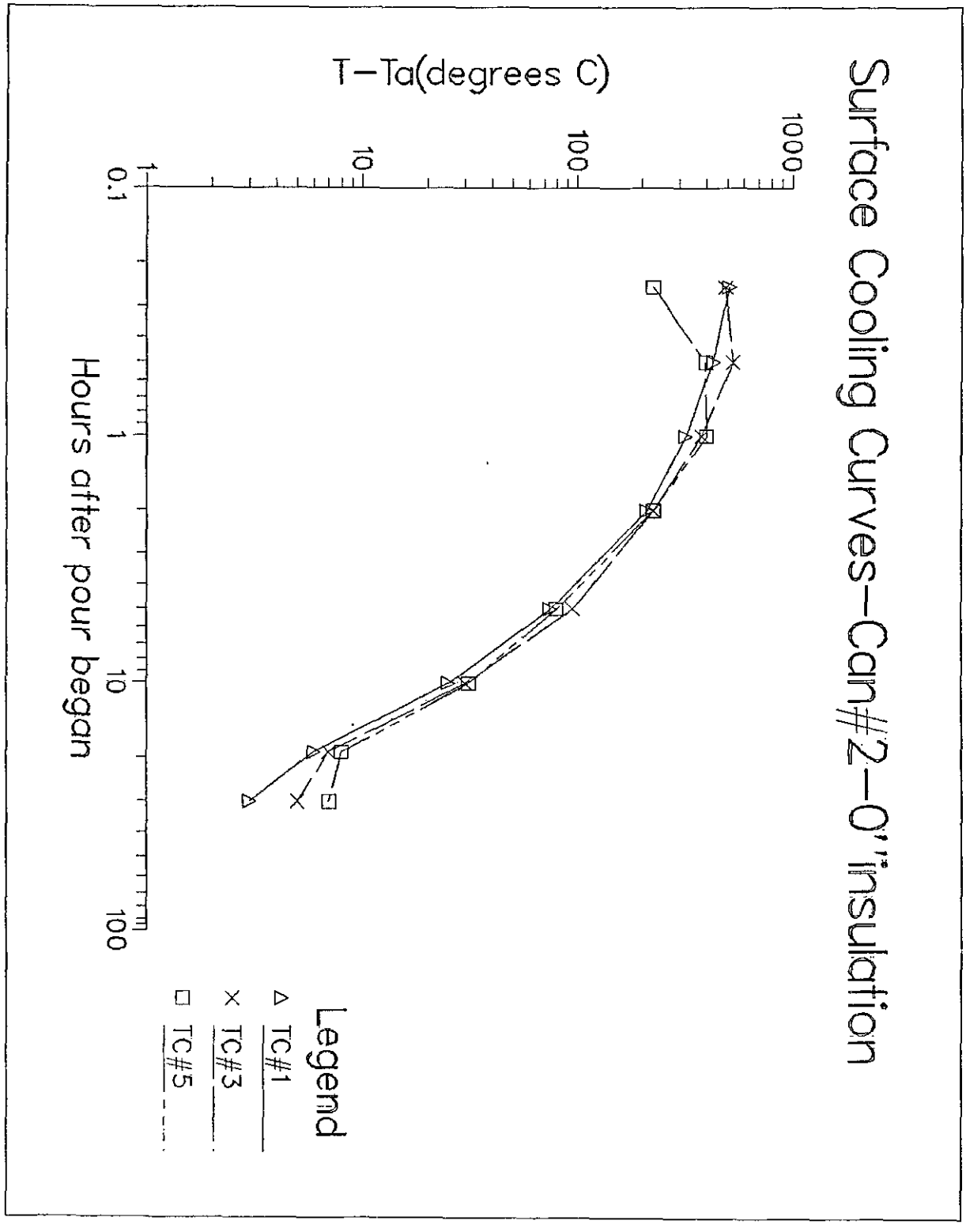
Surface Cooling Curves—Can#2—0" insulation
T—Ta(degrees C)
1000
100
10
1
0.1
Hours after pour began
1
10
100
Legend
TC#1
TC#3
TC#5

FIGURE 5

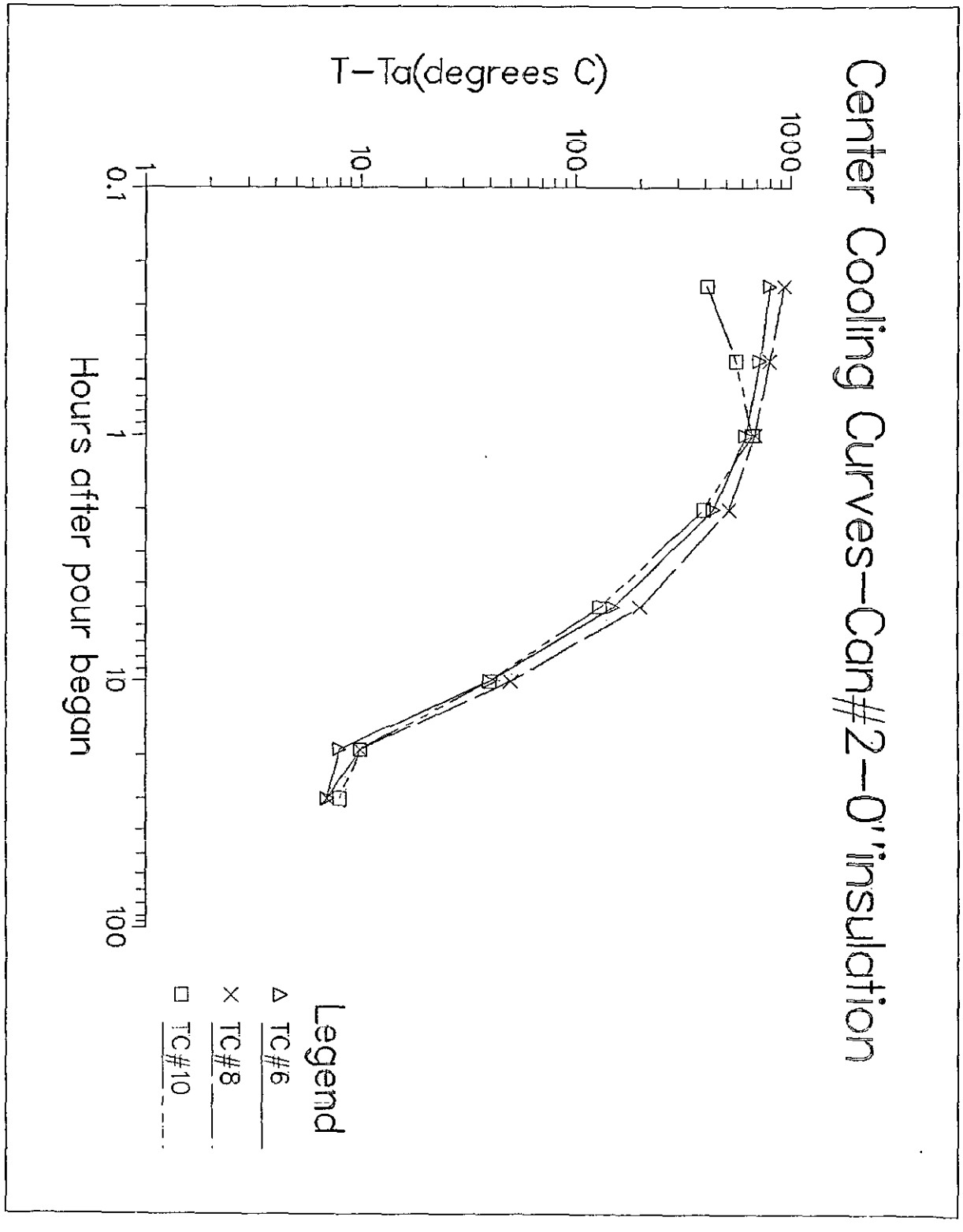
Center Cooling Curves–Can#2–0"insulation
T–Ta(degrees C)
1000
100
10
1
0.1
Hours after pour began
1
10
100
Legend
TC#6
TC#8
TC#10

FIGURE 6

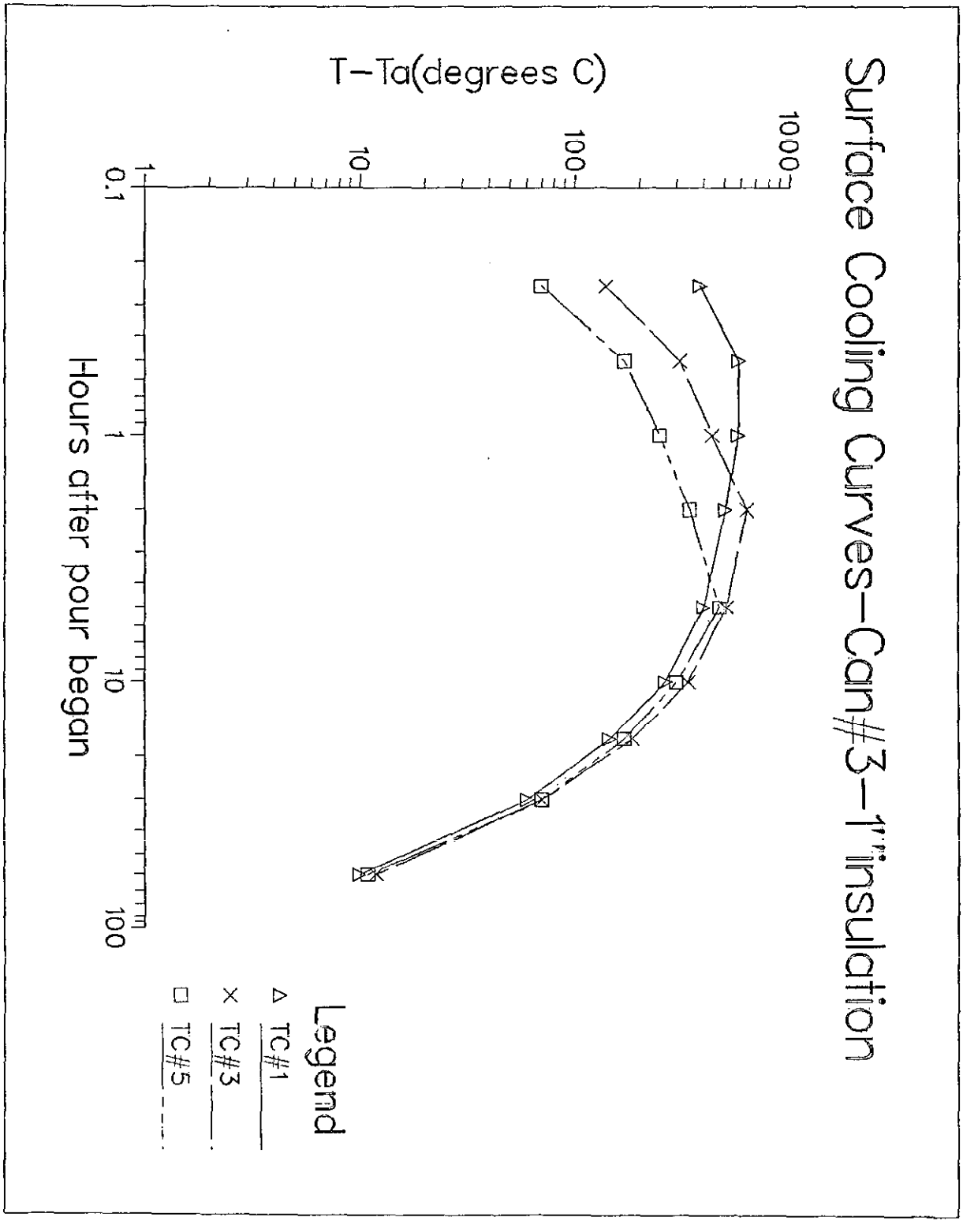
Surface Cooling Curves–Can#3–1"insulation
T–Ta(degrees C)
1000
100
10
1
0.1
Hours after pour began
1
10
100
Legend
TC#1
TC#3
TC#5

FIGURE 7

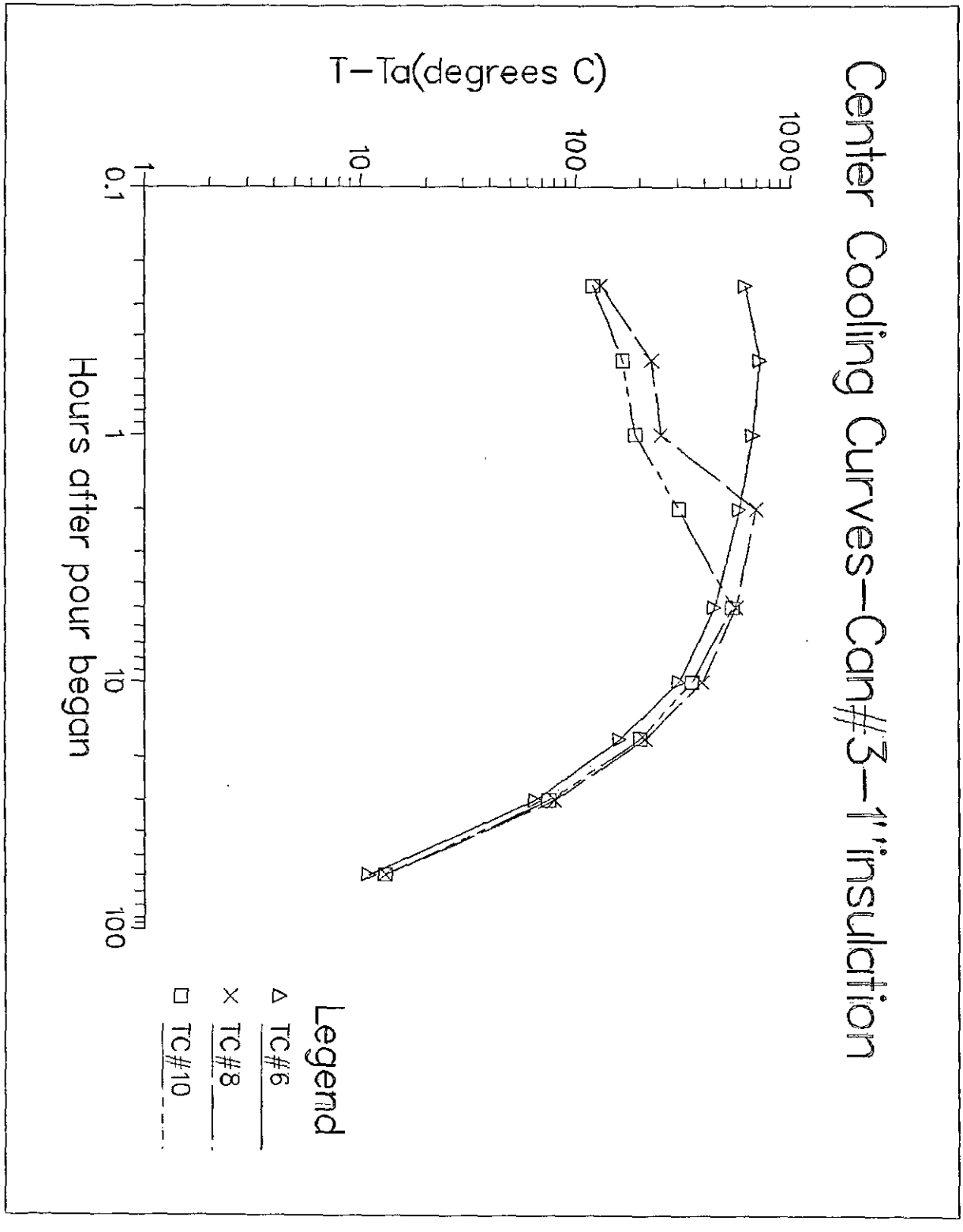
Center Cooling Curves—Can#3—1" insulation
T—Ta(degrees C)
1000
100
10
1
0.1
Hours after pour began
1
10
100
Legend
TC#6
TC#8
TC#10

FIGURE 8

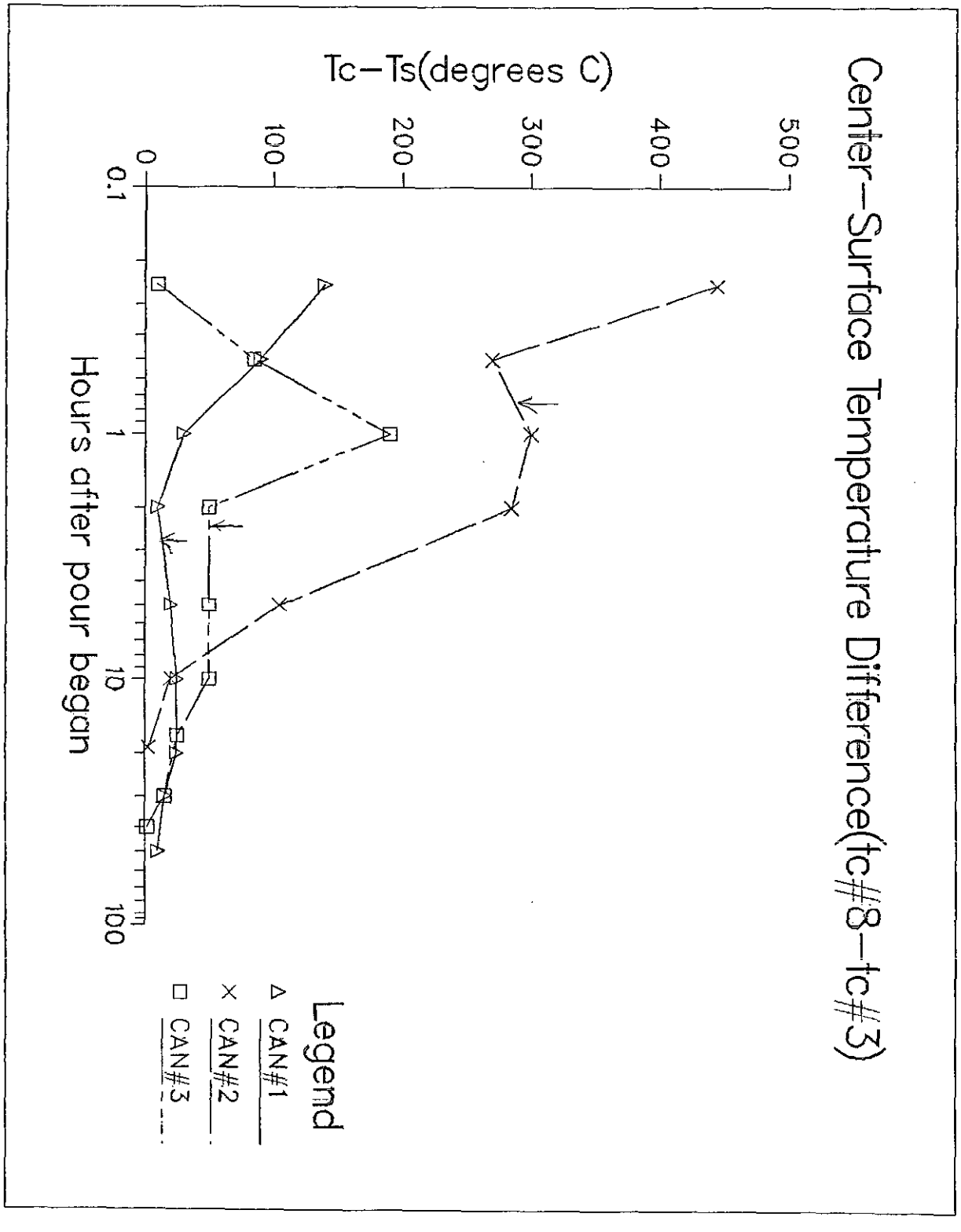
Center-Surface Temperature Difference(tc#8-tc#3)
Tc-Ts(degrees C)
500
400
300
200
100
0
0.1
1
10
100
Hours after pour began
Legend
CAN#1
CAN#2
CAN#3

FIGURE 9

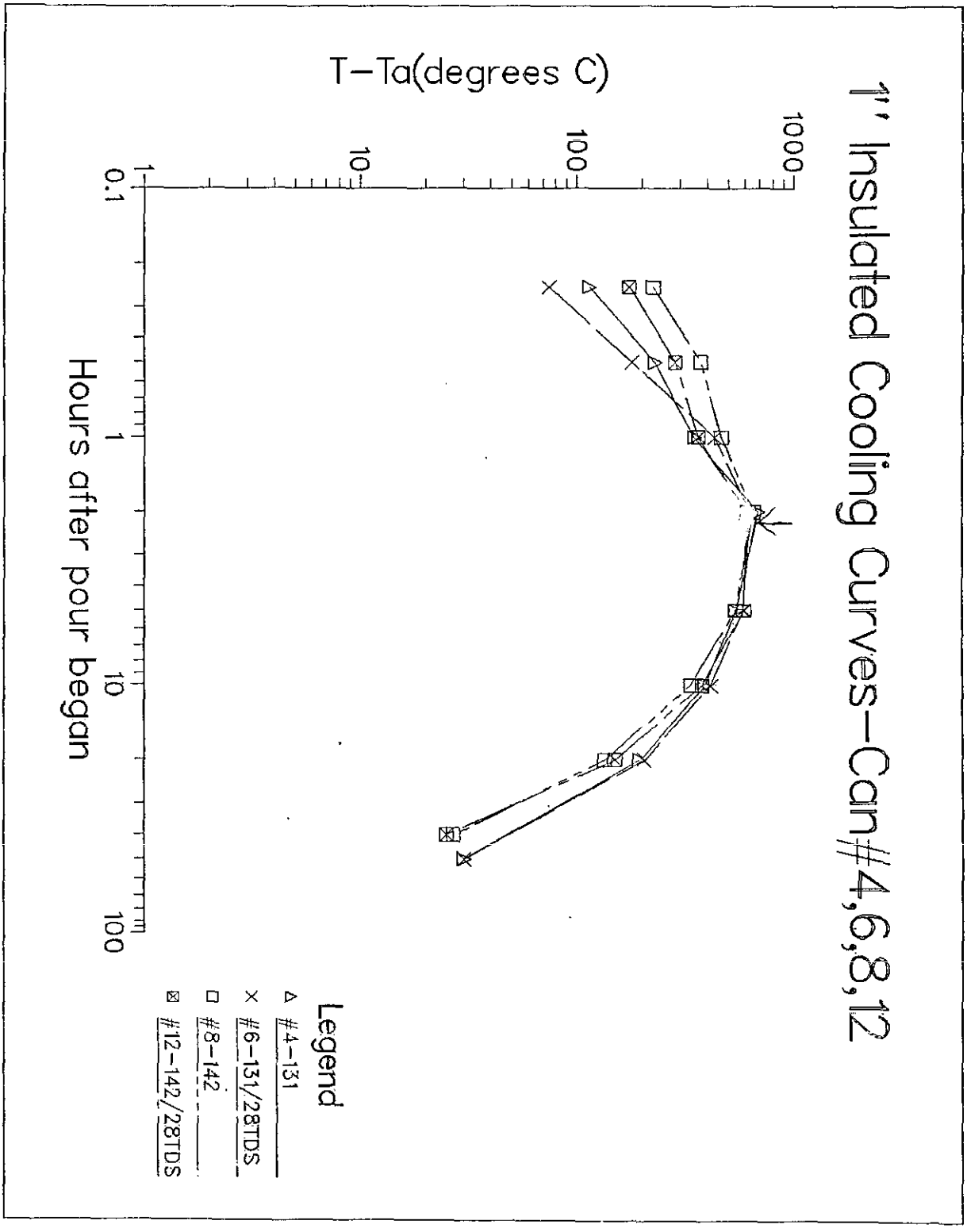
1" Insulated Cooling Curves-Can#4,6,8,12
T-Ta(degrees C)
1000
100
10
1
0.1
Hours after pour began
1
10
100
Legend
#4-131
#6-131/28TDS
#8-142
#12-142/28TDS

FIGURE 10

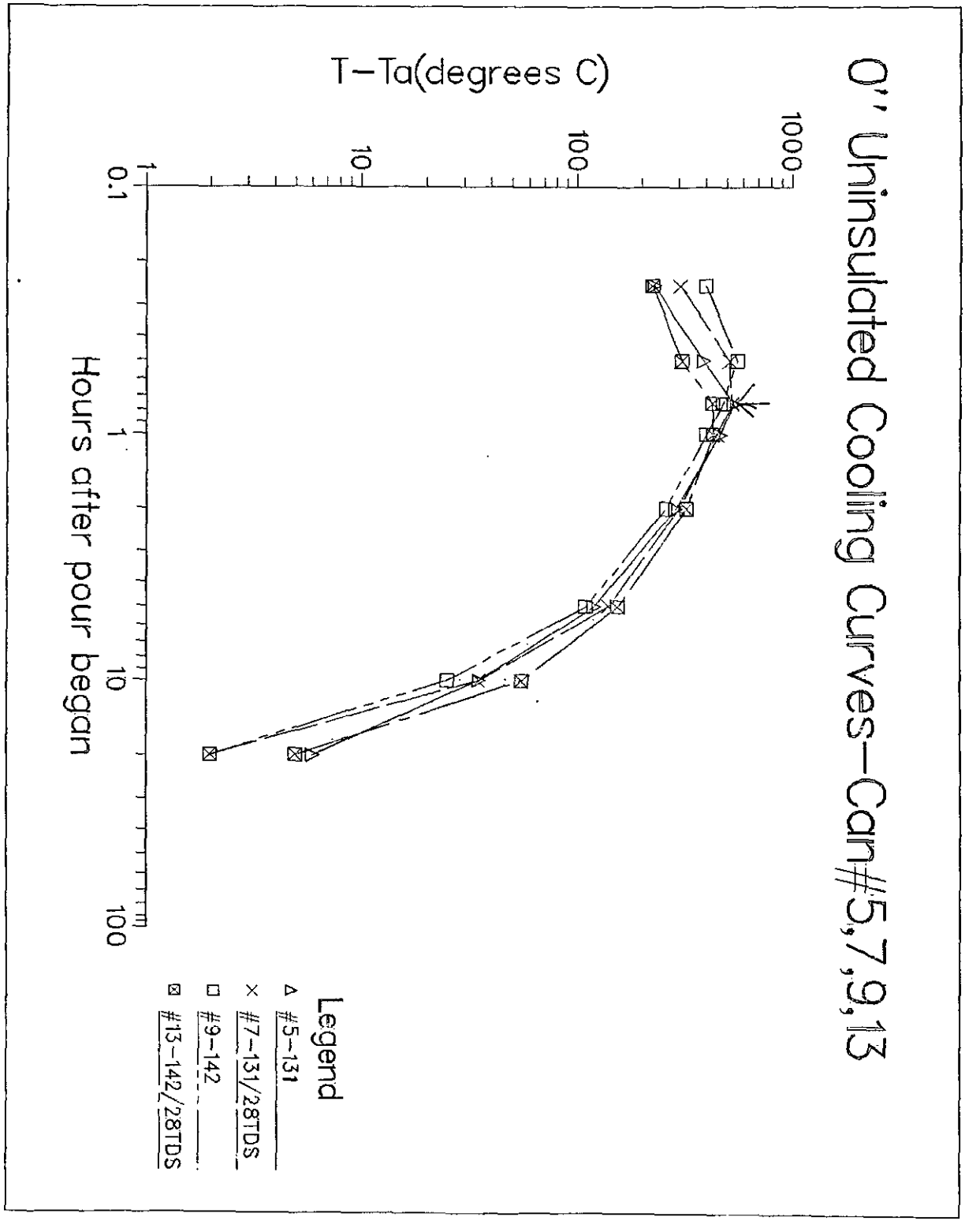
0'' Uninsulated Cooling Curves—Can#5,7,9,13
T−Ta(degrees C)
1000
100
10
1
0.1
Hours after pour began
1
10
100
Legend
#5−131
#7−131/28TDS
#9−142
#13−142/28TDS

FIGURE 11

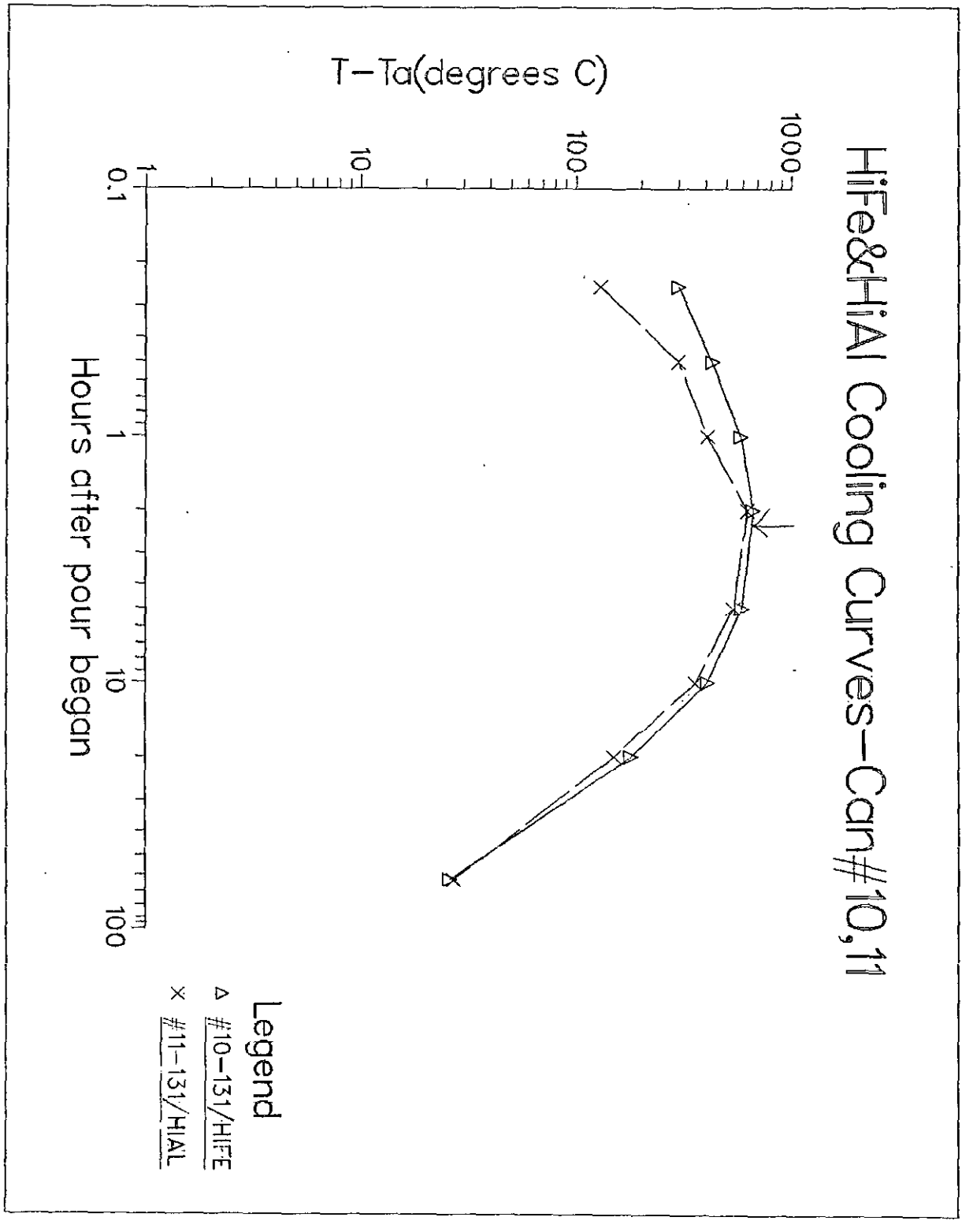
HiFe&HiAl Cooling Curves—Can#10,11
T—Ta(degrees C)
1000
100
10
1
0.1
Hours after pour began
1
10
100
Legend
Δ #10—131/HIFE
× #11—131/HIAL

FIGURE 12

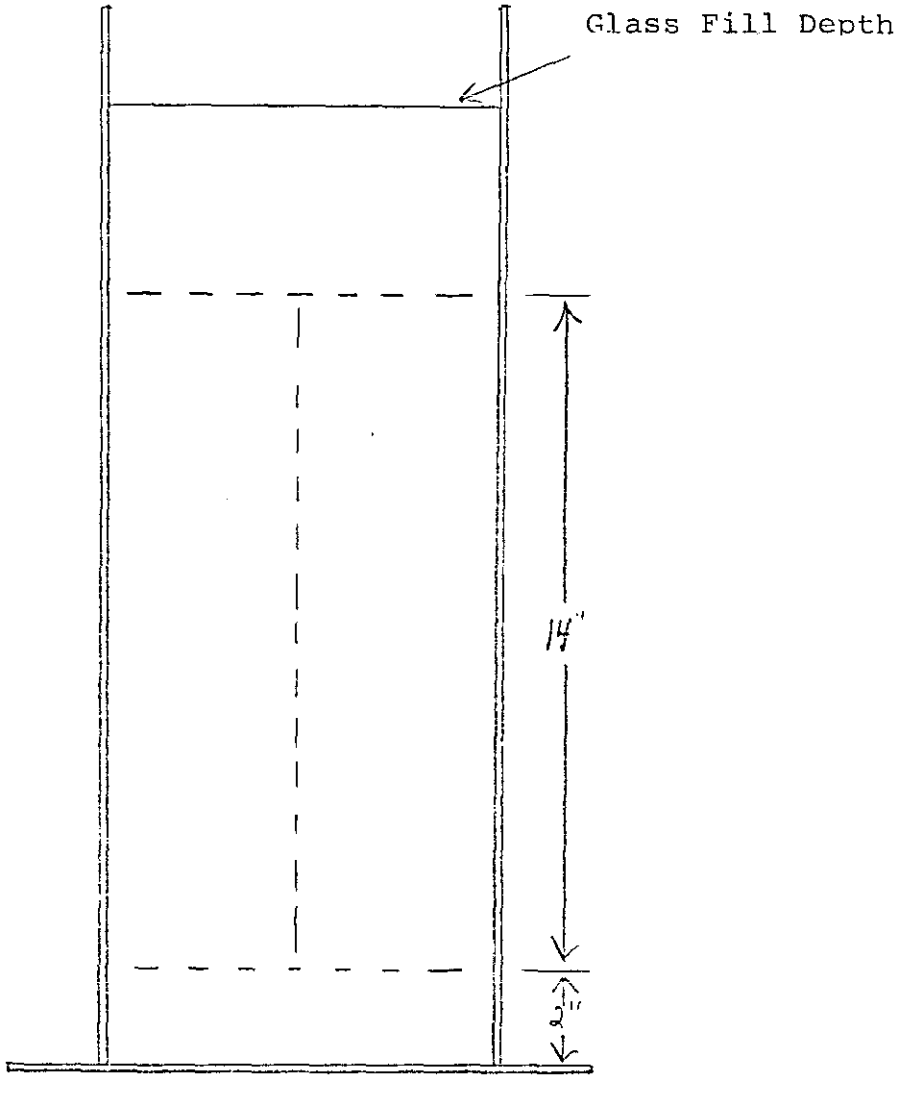

FIGURE 13. Canister Sectioning

FIGURE 14

Canister #6 Voids